GASIFICATION KINETICS OF ULTRAFINE COAL CHAR OXIDATION IN FLAME REACTIONS

G.R. John and I.S.N. Mkilaha
University of Dar es Salaam, Department of Energy Engineering
P.O. Box 35131, DSM, Tanzania, Email: grkjohn@uccmail.co.tz

ABSTRACT

Pulverized coal combustion is exceedingly complex with a vast number of variables. In order to avoid the complications associated with the burning of coal char, a controlled study has been made of the oxidation of fine graphite in laminar methane-air flame as a contribution to the understanding of the more complex phenomena of the gasification kinetics of the char. The burning of methane is equivalent to the burning of volatiles and graphite oxidation is similar to that of coal char. Aspects of this have been simulated in experimental and computational studies of 4μm diameter graphite particle burning in methane – air flames at a pressure of 0.160 atm. The low pressure not only ensured good spatial resolution of the flame structure but it also ensured that the graphite reaction rate was chemically controlled.

Comparable values from prediction and measurements were observed and were explainable in terms of the presence of reactive flame radicals O, OH, and H in controlling oxidation aided by the catalytic radicals attack by molecular oxygen. The primary oxidation product from the kinetics is CO. This is simultaneously coupled to a detailed multi-step gas phase kinetic mechanism in the oxidation for CH_4 – air flames. For lean flames, the available CO in the presence of the reactive radicals enhances reactions with the effect of enhancing the associated heat release rate. This contributes to the observed enhanced burning velocities in these flames. For rich flames, because of the limited amounts of O_2, the catalytic effect is impaired and thus reduces the char oxidation rate and thus reduces the burning velocity of the propagating flame.

1. INTRODUCTION

The kinetic modeling of coal gasification is fraught with difficulties due to the extreme complexity of the phenomena. In a phased approach to the problem an attempt is made to simulate ultra-fine coal gasification with that of ultra fine graphite gasification in methane – air flame. This is based on the assumption that the gas devolatilised from the coal is methane and the rate of devolatilisation is expressed by a rate equation that is part of the complex of chemical reactions and the mixing of the volatiles with the surrounding air is instantaneous. Ultra-fine is so fine that thermal and velocity lags are to be neglected. It is a limit condition, closely shown for particles sizes of 5 μm but less so as diameters tend to 20 μm (Bradley et al, 1986, John, 1995). Coal char combustion was simulated by burning graphite in methane-air flames. The burning of methane is equivalent to the burning of volatiles and graphite oxidation is similar to that of coal char. The philosophy of this adaptability has been reported in the work by Bradley et al., 1994. Combustion characteristics of these particle sizes are chemically controlled (Bradley and Lee, 1984). The deployment of ultra fine particles is of practical interest in that ultra-fine coal of up to 10μm means particle size has been shown to be oxidised completely in flames. These are capable of producing a hotter, shorter flame compared to normal pulverized coal and might be deployed in systems originally designed for residual fuel oil (Barrat and Roberts, 1989). This approach has been applied with some success to calculate lean flammability limits and burning velocities of some coal – air flames (Bradley et al, 1989). Investigations at high levels of concentrations of particles may elucidate the kinetics of actual coal char gasification in flames. This paper reports on both the experimentally and theoretically obtained findings in that direction.

2. SIMULATED COAL-GRAPHITE COMBUSTION

Coal devolatilises upon heating, and the methane - air graphite model is modified to take account of the rate of this. It is assumed that devolatilisation produces volatile and residual solid matter: the former consisting

solely of methane and the latter solely of carbon. Mixing of methane and the surrounding air is rapid and the methane burns in a premixed methane - air flame, the kinetics of which are coupled with those for graphite oxidation. The solid char is assumed to have the same effect in the coal - air flame as graphite has in the methane - air - graphite flame, Bradley et al. (1989). In the present studies, the char oxidation model of Dixon - Lewis et al (1991) and the two flux radiative energy model of Chen (1990) are deployed in the oxidation model.

2.1 Volatile Composition, Chemical and Devolatilisation Kinetics

2.1.1 Volatile Composition

The chemical composition of the volatiles depends upon that of the coal, the temperature, and the rate of heating. The review of gaseous volatiles composition by Bradley et al. (1986) showed the dominant volatiles for most coals to be CO_2, CO, CH_4, H_2, H_2O and C_2H_4. For younger coals, Bradley et al. (1991) reviewed the findings of several researchers and suggested the major constituents to be C_2H_4, CO, C_2H_2, CH_4, CO_2, H_2O and H_2. Though the volatile composition is diverse, in modelling the number of constituents has usually been reduced. In the coal - air flame model of Smoot and Smith (1990), volatile products were assumed to consist of CO, H_2, N_2, OH and unnamed hydrocarbon C_nH_m. Although Bradley et al. (1991) found nine major volatile constituents of Sinai coal, in modeling the flame propagation for this coal only six constituents were considered. These were C_2H_4, CO, CH_4, CO_2, H_2. In their model, Dixon - Lewis et al (1987) and Bradley et al (1989) assumed CH_4 to be the sole volatile. This assumption is also made in the present work. Again, it is assumed that the remaining solid after devolatilisation is a char consisting entirely of carbon.

The amount of volatiles actually released at the high heating rates and temperatures of real furnaces is greater than that determined in a proximate analysis of volatile matter (VM). The evolved VM is assumed to be increased by some not entirely determinate amount over that given by the proximate analysis. Williams et al (2001) have estimated that the actual VM increased from the proximate value of 35 - 40 % for bituminous coals to 50 - 60 %. Ruksana (2000) suggested that this increase is 20 % for high bituminous volatile coals. In this work no such factor is introduced.

2.1.2 Devolatilisation Kinetics and Rate of Char burn up

Current devolatilisation kinetics generally assume the process to be chemically rate - controlled (Ruksana, 2000). Due to the complexity of the process, it is still impossible to formulate a rigorous kinetic model of devolatilisation and controversy surrounds the experimental determination of kinetic parameters, Williams et al (2001). At high temperatures, devolatilisation is extremely rapid, thus forcing most experimental investigations into a narrow temperature range, (**ibid**). The determination of kinetic parameters over a narrow temperature range necessarily introduces uncertainty about the use of such parameters as activation energy over a wider range.

Irrespect of these difficulties, attempts have been made to correlate reaction rates and other physiochemical parameters. William et al. (2001) suggest the use of the simplest form of first order kinetics, because this can fit the data as satisfactorily as some of the more complex formulations. On this account, and with the assumption that the volatiles consist only of methane, the devolatilisation kinetics have been presented by Dixon - Lewis et al (1987), Bradley et al (1989) and William et al (2001) by the simple chemical equation:

$$CH_{4,solid} \rightarrow CH_{4,gas} \qquad (1)$$

The endothermicity associated with devolatilisation, assumed to be temperature independent, was 1724 kJ per kg CH_4 released, Dixon - Lewis et al (1987). The rate of devolatilisation is given by a first order molar rate, R_{CH_4} (Bradley et al 1989):

$$R_{CH_4} = k_{dev}\rho_g \frac{\frac{Y_m}{m_{CH_4}}}{(1-Y_c-Y_m)} kmole\ m^{-3}s^{-1} \qquad (2)$$

in which k_{dev} is a first order rate coefficient, ρ_g the gas phase density, m_{CH4} the molecular mass of methane, Y_m the mass fraction of combined methane held in the coal and Y_c the mass fraction of char in the total mixture The first order rate coefficient is that assigned the following value by Dixon - Lewis et al (1987);

$$k_{dev} = 10^{13} \exp(-21649/T)\ kmole^{-1}s^{-1} \qquad (3)$$

where T is the particle temperature. The subsequent gas phase kinetics for the combustion of volatiles are those for methane oxidation. The residence time of the char particles in the flame is short and it is assumed, as for graphite particles in methane - air flames, that the surface of any pores that develop in the char particles does not support oxidation. This is likely to be less valid than the comparable assumption for graphite. The oxidation of the char and the coupling of char and gas phase kinetics is treated in the same way as the oxidation of graphite in methane - air flames.

It is worth noting that in real turbulent pulverised coal flames, this coupling is of interest for the modelling of the near burner combustion (Ruksana, 2000). In this zone, because of the recirculation, the char residence time is increased. This should augment its oxidation via the radical species OH, O and H, that arise from the combustion of the volatiles in this zone (Williams et al, 2001). The CO resulting from the char oxidation would participate in the gas phase combustion and it is upon this combustion that the stability of the flame depends (**ibid**).

When the coupled char oxidation is incorporated into the models of pulverised coal combustion at 1.0 atm. pressure, as distinct from the low pressure of the present graphite flames, assumptions that the reaction is chemically, and not diffusion, controlled are only valid for particle sizes less than 10 μm (John, 1995). The computational studies of John (1995) showed that at 1.0 atm., the reaction rates of poreless carbon particles of less than this size were chemically controlled at temperatures below 2000 K. As the size increased from 10 to 120 μm there was a transition from chemical to diffusion control. Such a wide band is explained by the different reaction kinetics and diffusion rates of different species. These studies are in general agreement with the predominantly experimental data collated by Bradley et al. (1994) where the upper particle size limit for chemically controlled burning of coal chars is 100 μm at 1.0 atm., at temperatures below 2500 K.

3. ANALYSIS OF GASIFICATION KINETICS

3.1 Experimental Arrangement and Gas phase kinetics

The experimental arrangement for the study of the gasification kinetics was undertaken in a low pressure burner, an apparatus set described else where (Bradley et al 1991). A schematic deployment of the system is depicted in Fig 1. Here, a gas flow system, enabled streams of methane – air and the same seeded with graphite to flow to the burner. This was used to infer the results of simulated ultrafine coal char gasification through the study of the structure of laminar flat methane – air flames seeded with graphite particles. Premixtures of methane, technical grade 100%, and air latter seeded with artificial graphite or alumina powder was employed. The artificial graphite powder had specific surface area 18.3 $m^2\ g^{-1}$, particle size ≤ 5 μm (95.5%), particle density (measured with mercury) 1.6 g cm^{-3}, porosity 0.3, SiO_2 0.013%, Al_2O3 0.0064%, Fe_2O_3 0.083%, CaO 0.0075%, TiO_2 0.0063%, MgO trace, moisture 0.2% ash 0.09%. The particle mean size diameter, measured with the laser based visibility technique was 4 μm. Gas temperature, gas velocities and species concentrations were studied in the flames at 0.160 atm using methane-air flames of equivalence ratios ϕ of 0.6 0.7, 1.07, 1.2. The equivalent ratio ϕ is expressed by

$$\phi = \frac{(m_{CH_4}/m_{air})Act}{(m_{CH_4}/m_{air})Stoich} \qquad (4)$$

where m_{CH4} is the mass of methane, m_{air}, mass of air, Act. is actual and stoich. is stoichiometric. The burning velocity was measured for all the equivalence ratios and different graphite loading. For species concentrations, the equivalence ratio of 0.7 and 1.2 were deployed, these represented the fuel

lean and fuel rich flames. In the experimental conditions, for each of the methane-air mixtures at the four equivalence ratios, four different amounts of graphite were added. It is of interest in the context of modelling the combustion of coal to express an equivalent mass fraction of volatile material, VM, the mass of methane to the mass of methane plus graphite of the initial reactants as:

$$VM = \frac{m_{CH_4}}{m_{CH_4} + m_c} \qquad (5)$$

where m_{CH_4} and m_c are the mass of methane and graphite respectively. The ratios used in the present work were 0.8, 0.6, 0.5 and 0.4 at 0.160 atm.

The introduced graphite particles in the methane – air flame are assumed to consist only of pore-less carbon whose oxidation process is chemically controlled (Mulcahy and Smith, 1969). This is valid for small carbon particles of less than 10 μm diameter, in 0.1 to 1.0 atm for temperature range between 500 K and 2500 K (Bradley et al ,1985). The oxidation rate coefficients are those taken from Mulcahy and Smith, (1969) and expressed as;

$$k_i = A_i T \exp(-E_i/RT) \qquad (6)$$

k_i is specific reaction rate in kg $m^{-2}s^{-1}$ atm^{-1}, A_i the pre-exponential factor, T absolute temperature, E_i the activation energy, R the universal gas constant.

In the schematic figure; Fig 1, V_1….V_4, V_p, V_c, V_a, V_B, V_i, V_f are flow control valves, R a rotameter whilst g and h are needle valves.

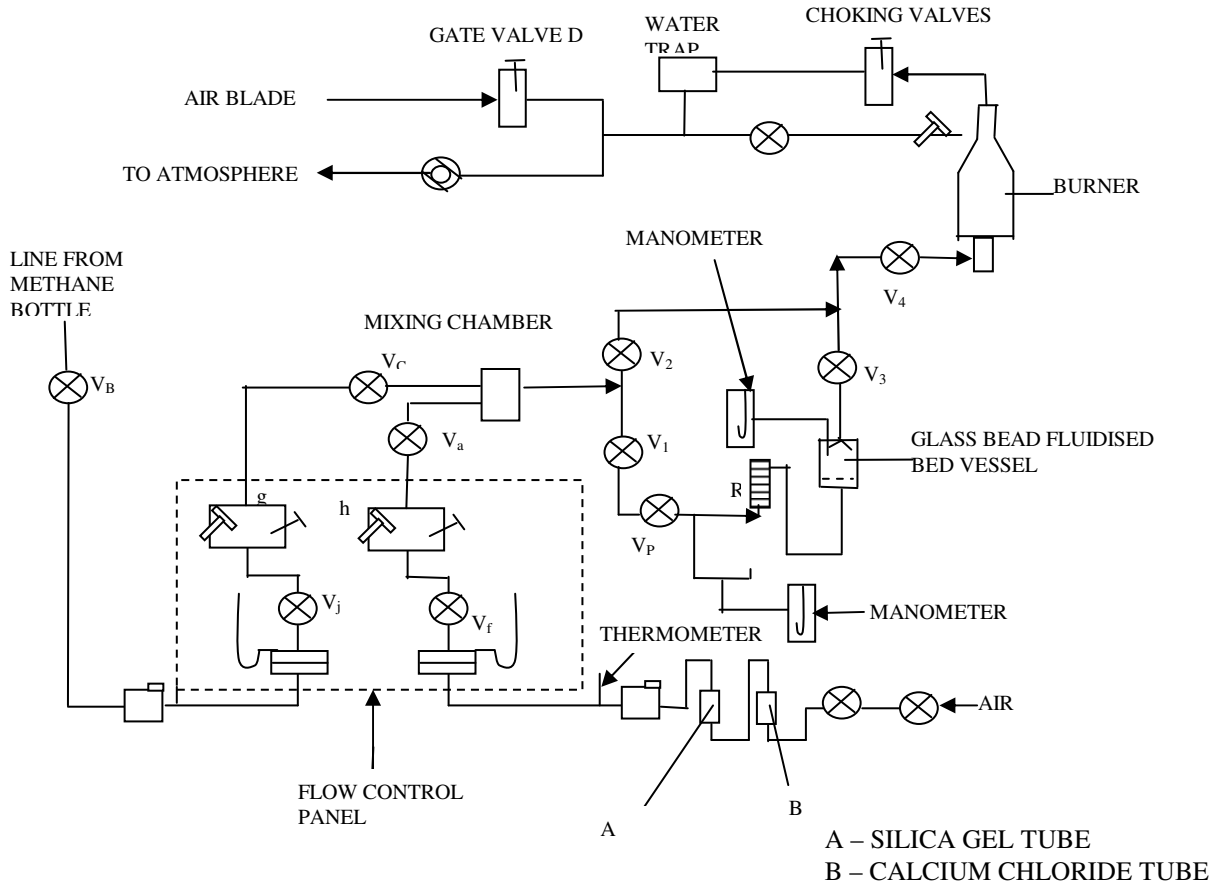

Fig 1 Carbon particles – Methane/Air gas Flow System

The methane-air gas phase kinetic reactions employed is available from Dixon-Lewis (1984) and given in Table 1. The coefficients of parameters for expressions in the forward rate and independent equilibrium constants are expressed as $k = AT^{B}exp(-C/T)$ and equilibrium constants as $K = DTEexp(F/T) = k_{forward}/k_{reverse}$ (Dixon et al, 1991), both in units of cm mole.s. The values of rate and equilibrium constants A, B, C,D and E and F for the different reactions are given in Table 1 (**ibid**). The scheme is necessary for the primary volatile combustion, here, methane (CH_4) in reaction steps 24-26. The responsible species for these exothermic reactions are H, O, OH radicals.

Table 1 Methane (CH_4) -Air Reaction Mechanism (Dixon-Lewis et al (1991)

No	Reaction	A	B	C/(K)	D	E	F/(K)
1	$OH + H_2 \leftrightarrow H_2O + H$	1.1×10^{9}	1.3	1825	0.21	0.0	-764
2	$H + O_2 \leftrightarrow OH + O$	1.8×10^{14}	0.0	8250	300.0	-0.372	8565
3	$O + H_2 \leftrightarrow OH + H$	1.8×10^{10}	1.0	4480	2.27	0.0	938
4	$H + O_2 + H_2 \leftrightarrow HO_2 + H_2$ $H + O_2 + N_2 \leftrightarrow HO_2 + N_2$ $H + O_2 + O_2 \leftrightarrow HO_2 + O_2$ $H + O_2 + H_2O \leftrightarrow HO_2 + HO_2$ $H + O_2 + CO \leftrightarrow HO_2 + CO$ $H + O_2 + CO_2 \leftrightarrow HO_2 + CO_2$ $H + O_2 + CH_3OH \leftrightarrow HO_2 + CH_3OH$	2.8×10^{18} 3.75×10^{20} 3.0×10^{20} 9.4×10^{18} 2.1×10^{18} 4.1×10^{18} 5.6×10^{18}	-0.86 -1.72 -1.72 -0.76 -0.86 -0.86 -0.86	0.0 0.0 0.0 0.0 0.0 0.0 0.0	0.7.45	0.0	-23380
5	$H + HO_2 \leftrightarrow OH + OH$	2.2×10^{14}	0.0	710			
6	$H + HO_2 \leftrightarrow O + O_2H$	2.2×10^{14}	0.0	710			
7	$H + HO_2 \leftrightarrow H_2 + O_2$	2.2×10^{14}	0.0	280			
8	$OH + HO_2 \leftrightarrow H_2O + O_2$	1.8×10^{13}	0.0	0.0			
9	$O + HO_2 \leftrightarrow OH + O_2$	2.0×10^{13}	0.0	0.0			
10	$H + H + H_2 \leftrightarrow H_2 + H_2$ $H + H + N_2 \leftrightarrow H_2 + N_2$ $H + H + O_2 \leftrightarrow H_2 + O_2$ $H + H + H_2O \leftrightarrow H_2 + H_2O$ $H + H + CO \leftrightarrow H_2 + CO$ $H + H + CO_2 \leftrightarrow H_2 + CO_2$ $H + H + CH_3OH \leftrightarrow H_2 + CH_3OH$	9.2×10^{16} 1.0×10^{18} 1.0×10^{18} 6.0×10^{19} 1.0×10^{18} 5.49×10^{20} 5.49×10^{20}	-0.6 -1.0 -1.0 -1.25 -1.0 -2.0 -2.0	0.0 0.0 0.0 0.0 0.0 0.0 0.0	0.24	0.0	-5259
11	$H + OH + M \leftrightarrow H_2O + M$ $M = H_2, O_2, CO, CO_2, CH_3OH,$ $M = H_2O$	1.6×10^{22} 8×10^{22}	-2.0 -2.0	0.0 0.0			
12	$H + O + M \leftrightarrow OH + M$ $M = H_2, O_2, CO, CO_2, CH_3OH,$ $M = H_2O$	6.2×10^{16} 3.1×10^{17}	-0.6 -0.6	0.0 0.0			
13	$OH + OH \leftrightarrow O + H_2$	K_{13}=exp. (27.1 + $1.5 \times 10^{-3} \times T$)					
14	$OH + CO \leftrightarrow CO_2 + H$	1.5×10^{7}	1.3	385	3.82×10^{-7}	1.19	-1306
15	$O + CO + M \leftrightarrow CO_2 + M$ $M = H_2, O_2, CO, CO_2, CH_3OH$ & H_2O	5.4×10^{15}	0.0	2300			
16	$H + CO + M \leftrightarrow CHO + M$ $M = H_2, O_2, CO, CO_2, CH_3OH$ & H_2O	5.0×10^{14}	0.0	755	1.7	0.0	-7080

17	$CHO + O_2 \leftrightarrow HO_2 + CO$	3.3×10^{13}	-0.4	0.0			
18	$CHO + H \leftrightarrow H_2 + CO$	1.2×10^{14}	0.0	0.0			
19	$CHO + OH \leftrightarrow H_2O + CO$	1.0×10^{14}	0.0	0.0			
20	$CHO + O \leftrightarrow OH + CO$	3.0×10^{13}					
21	$CH_2O + H \leftrightarrow CHO + H_2$	1×10^{4}	3.0	700	10.6	0.0	-7778
22	$CH_2O + OH \leftrightarrow CHO + H_2O$	3×10^{13}	0.0	600			
23	$CH_2O + O \leftrightarrow CHO + OH$	1.8×10^{13}	0.0	1540			
24	$CH_4 + H \leftrightarrow CH_3 + H_2$	2.2×10^{4}	3.0	4400	29.3	0.0	355
25	$CH_4 + OH \leftrightarrow CH_3 + H_2O$	1.6×10^{7}	1.83	1400	6.153	0.0	-7285
26	$CH_4 + O \leftrightarrow CH_3 + OH$	1.2×10^{7}	2.1	3840	66.51	0.0	1293
27	$CH_3 + O \leftrightarrow CH_2O + H_2$	7.0×10^{13}	0.0	0.0	.07228	0.0	-35100

3.2 Char Oxidation

The theoretical and experimental studies by Bradley et al (1989) on external surface reaction rates for graphite particles of the size referred in this investigation in methane – air flames, albeit at lean equivalence ratios revealed the rates to be greatest in the flame reaction zone. It was observed that the oxidation, initially believed to be due to O, OH and H rather than other species was refuted on the ground that the gas phase concentrations of these were not adequate to explain the observed carbon reaction rates, Dixon – Lewis et al (1991). Pore reaction contribution would be unlikely due to limited residence time of particles in the flame (Bradley et al, 1985).

A plausible explanation of the high oxidation rates lay on the ability of O, H, and OH to catalyse reaction of C and oxygen molecules on or near the char surface. This phenomenon have been observed and accounted for in the attach of C by the species in the presence of O_2, Mulcaly and Smith (1969). Accordingly, an overall reaction of the form shown in the reaction equation no 7 is suggested;

$$H + 2C + O_2 \longrightarrow 2CO + H \qquad (7)$$

With this reaction, a possible reaction scheme at or near the carbon surface of the form presented in Table 2 is pro-pounded. The radicals OH, O and H would be produced by reactions (28) to (31). These would react with carbon in reaction (34) and (36).

When the gas kinetic theory is evoked and ε_i is the surface collision efficiency for removal of a carbon atom at each successful collision, the collision rate Z_i, for species i, per unit of smooth particle envelope area (Dixon Lewis et al, 1991) is;

$$Z_i = 4.43 \times 10^5 \, p_{i,s}/(Tm_i)^{0.5} \text{ mol m}^{-2} \text{ s}^{-1} \qquad (8)$$

$p_{i,s}$ is surface pressure in atmospheres, T absolute temperature and m_i the molecular mass. Then, the rate of carbon oxidation arising from the collision becomes F_i, (**ibid**) such that;

$$F_i = 12x10^{-3} \in_i Z_i \qquad (9)$$

$$= 5320 \in_i p_{i,s}/(Tm_i)^{0.5} \text{ kg m}^{-2}\text{s}^{-1}$$

where $\in_i$ is the collision efficiency, Z_i, $P_{i,s}$ and $_{Tm,i}$ as defined earlier. This assumes one carbon atom is oxidised at each successful collision (**ibid**). For H, OH, O and O_2 collisions and at a gas of temperature, of T_g, these carbon fluxes are, respectively (**ibid**) in kg m^{-2} s^{-1};

$$F_H = 5320 \in_H p_{H,s} T_g^{-0.5} \qquad (10a)$$

$$F_{OH} = 1290 \in_{OH} p_{OH,s} T_g^{-0.5} \qquad (10b)$$

$$F_O = 1330 \in_O p_{O,s} T_g^{-0.5} \qquad (10c)$$

$$F_{O2} = 1880 \in_{O2} p_{O2,s} T_g^{-0.5} \qquad (10d)$$

Where F and $\in_i$ as defined earlier, $P_{i,s}$ assumes the nomenclature for partial surface pressures of H, OH, O and O_2 and T_g is the equilibrium gas temperature.

The value of the collision efficiency for oxygen molecules shall be that suggested by Dixon Lewis et al (1991) $\in_{O2} = k_{char}$ [H] with kchar =

5.5. x 10^4 m^3 k $mole^{-1}$. The other efficiencies $\in_H$, $\in_{OH}$, $\in_O$ were temperature independent and assigned values proposed by Bradley et al (1985) as 0.036, 0.28 and 0.5 respectively.

The primary product arising from the surface reaction is CO, the oxidation of which is coupled simultaneously with the multi-step methane-oxidation kinetic scheme given in Table 1. Accurate validation of predicted and measured burning velocities necessitated the introduction of a kinetic reaction for a carbon surface recombination reaction (Reaction 38, Table 2), presented by Backreedy et al (2002) and Dixon Lewis et al (1991) in the form;

$$H + OH + C \rightarrow H_2O + C \qquad (11)$$

with a temperature independent rate coefficient, k_r = 1.1 x 10^7 m^4 $kmol^{-1}$ s^{-1} (Dixon-Lewis et al, 1991). The resulting volumetric molar rate of recombination R_{H2O} of H and OH (**ibid**) is;

$$R_{H_2O} = k_r \rho^2{}_m \sigma_{OH} \sigma_H A_s \qquad (12)$$

k_r is the rate constant, ρ_m the molar density, σ_{OH} and σ_H the mole fraction of OH and H in the mixture and A_s is total external surface area of graphite particles in a unit volume of the mixture.

No	Reaction	Δ H kJ g^{-1} C burnt	Rate of carbon oxidation F_i, or Rate parameter
(28)	H + O_2 + C ↔ HO_2 + C	-	Reaction (37),
(29)	HO_2 + H ↔ OH + OH	-	Reaction (5), Table 1
(30)	HO_2 + H ↔O + H2O	-	Reaction (6), Table 1
(31)	CO + OH ↔CO_2 + H	-	Reaction (14), Table 1
(32)	CH + O_2 ↔ CHO + O	-	Reaction (37),
(33)	CHO + O_2 ↔ CO + HO_2	-	Reaction (17), Table 1
(34)	C + H ↔ CH	-24.4	Eq. (3a)
(35)	C + OH ↔ CO + H	6.8	Eq. (3b)
(36)	C + O ↔ CO	-28.17	Eq. (3c)
(37)	H + 2C + O_2 ↔2CO + H	-8.0	Eq. (3d)

No	Reaction	Rate constant, k_r, (m^4 $kmole^{-1}s^{-1}$)
(38)	H + OH + C ↔ H_2O + C	1.1 x 10^7

Table 2 Possible catalytic mechanisms at or near the carbon surface (Reaction 28 to 37) and surface recombination at the surface of carbon, Reaction 38.

4. COMPUTATIONAL AND RESULTS ANALYSIS

4.1 Computational Analysis

With the various aspects presented, and by considering the experimental unidirectional flame in the x-direction, a set of time dependent, conservation equation in the flame flow for the two – phase system was considered for gaseous species (molar rates) mass conservation and energy conservation;

(i) Gaseous species (molar rates)

$$\rho t \frac{\partial(F\sigma_{ig})}{\partial t} + M \frac{\partial(F\sigma_{ig})}{\partial x} = -\frac{\partial(j_i / m_i)}{\partial x} + R_i \qquad (13)$$

(ii) Mass conservation - solid graphite species, (mass rate)

$$\rho_t \frac{\partial Y_c}{\partial t} + M \frac{\partial Y_c}{\partial x} = m_c R_c \qquad (14)$$

(iii) Energy conservation (specific enthalpy, h)

$$\rho_t \frac{\partial h}{\partial t} + M \frac{\partial h}{\partial x} = -\frac{\partial(q_d + q_c + q_r)}{\partial x} \qquad (15)$$

Y_c is graphite/carbon mass fraction in the overall mixture, subscript g denotes mass fraction in the gas phase alone, t denotes value for the overall mixture and Y_i represents a species mass fraction. F = 1-Y_c, $\rho_g = F\rho_t$, ρ is the local mass density, M the total mass flux, j_i is the mass diffusive flux of species i, R_i is its volumetric molar rate of formation and m_i is its molecular mass. q_d, q_c and q_r are mass fluxes due to diffusion, thermal conduction and radiation respectively, $\sigma_{ig} = \frac{Y_{ig}}{m_i}$ represents the gaseous molar fractions. The volumetric molar

rate of graphite oxidation R_c in Eq. (14) is given as (John, 2005);

$$R_c = N \frac{\sum_{i=1}^{n} F_i}{m_c} A_p \qquad (16)$$

$\sum_{i=}^{n} F_i$ is the total rate of oxidation per unit external surface area of the particle, obtained from Eqs (10a) to (10d), m_c the molecular mass of carbon, N particle number density and A_p the external surface area of a single particle. Since ρ_t and ρ_g are the mass of mixture and gas in a unit volume respectively, then $(\rho_t - \rho_g) / m_p$ becomes the particle number density, N. When this is evoked for Eq. (16) with $\rho_g = F\rho_t$ then R_c is

$$R_{cc} = 6\rho_g \frac{1-F}{F} \frac{\sum_{i=}^{n} F_i}{m_c} \frac{1}{\rho_p d_x} \qquad (17)$$

d_x is graphite particle diameter at a position x and ρ_p the particle density. The particles were assumed to be spherical and of a constant density of 1600 kgm^{-3} at all temperatures, Bradley et al (1991). The specific heat of graphite was assumed to be temperature independent and equal to 1.5 $Jg^{-1}\ k^{-1}$ (Dixon – Lewis et al, 1991). Gaseous specific heats and enthalpies were expressed as polynomial functions of temperatures, (Dixon – Lewis 1984), following the JANAF Thermochemical Tables (1977) and NASA Thermochemical Polynomial Tables (1984).

Detailed transport formulation for thermal conduction flux, q_c, and thermal diffusion, q_d are in accordance with those deployed by John (2005). For computational economy, only H, N_2, O_2, H_2, CO, CO_2, H_2O and CH_4, which are predominant in coal combustion, (Backreedy et al, 2002) were included in the calculation of the thermal conductivity. The expression for radiative flux q_r, together with a combustion mathematical model formulated and described by Chen (1990) and John (1991) were deployed to give corresponding model predictions.

4.2 Analysis of Results

4.2.1 The Influence of Graphite Reactions

The measured and computed values of the laminar burning velocities at different values of mass of volatile to the total mass of the mixture, F_c, is displayed in Fig. 2. The computed values are the curves and the measured values the symbols. In general, computed values are greater than those measured, and the discrepancy increases with equivalence ratio. For a methane – air equivalence ratio of 0.6 the increase in the burning velocity, u_υ, is uniformly maintained with increase in F_c. For 1.2 the elevation is almost constant, whatever the value of F_c. ϕ = 0.6 and F_c = 0.04 correspond to an overall equivalence ratio, ϕ_o = 1.07. Clearly, there is some difficulty in accurately modelling the overall rich flames. Two factors might explain the increased computed values of u_υ, one is the suppression of radial velocity in the model and the other is that at higher values of F_c there is an inevitable loss of energy by radiating hot flame particles to the burner matrix with a consequence of reduced heat release rate. This reduces the burning velocity (John, 2005).

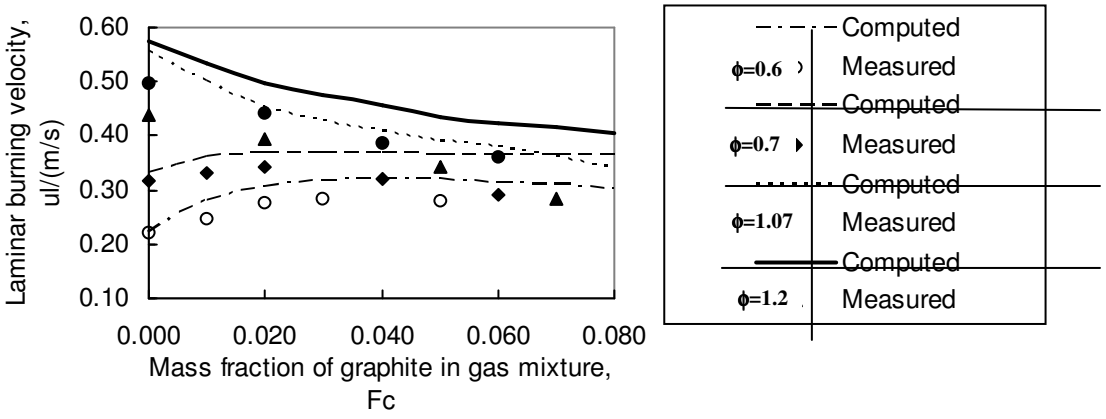

Fig 2 Variation of laminar burning velocity with graphite mass ratio in gas mixture, F, for different methane-air flames of equivalent ratio ϕ; 0.6, 0.7, 1.07, 1.2 at 0.160 atm.

Profiles of dry molar percentages of CO, CO_2, and O_2 are shown in Figs. 3 to 6. Because of space, these are shown only for initially lean flame (ϕ = 0.7) and rich flame (ϕ = 1.2). These concentrations are well predicted by the model at all graphite mass ratios for the initially lean CH_4 – air flames. For the initially rich flames, the model predicts well the concentrations of CO and that of CO_2. However, it is noticeable that for all values of F_c at ϕ = 1.2 the rate of reaction of O_2 is over predicted.

Despite these limitations, the model predicts the flame structure and burning velocities fairly well.

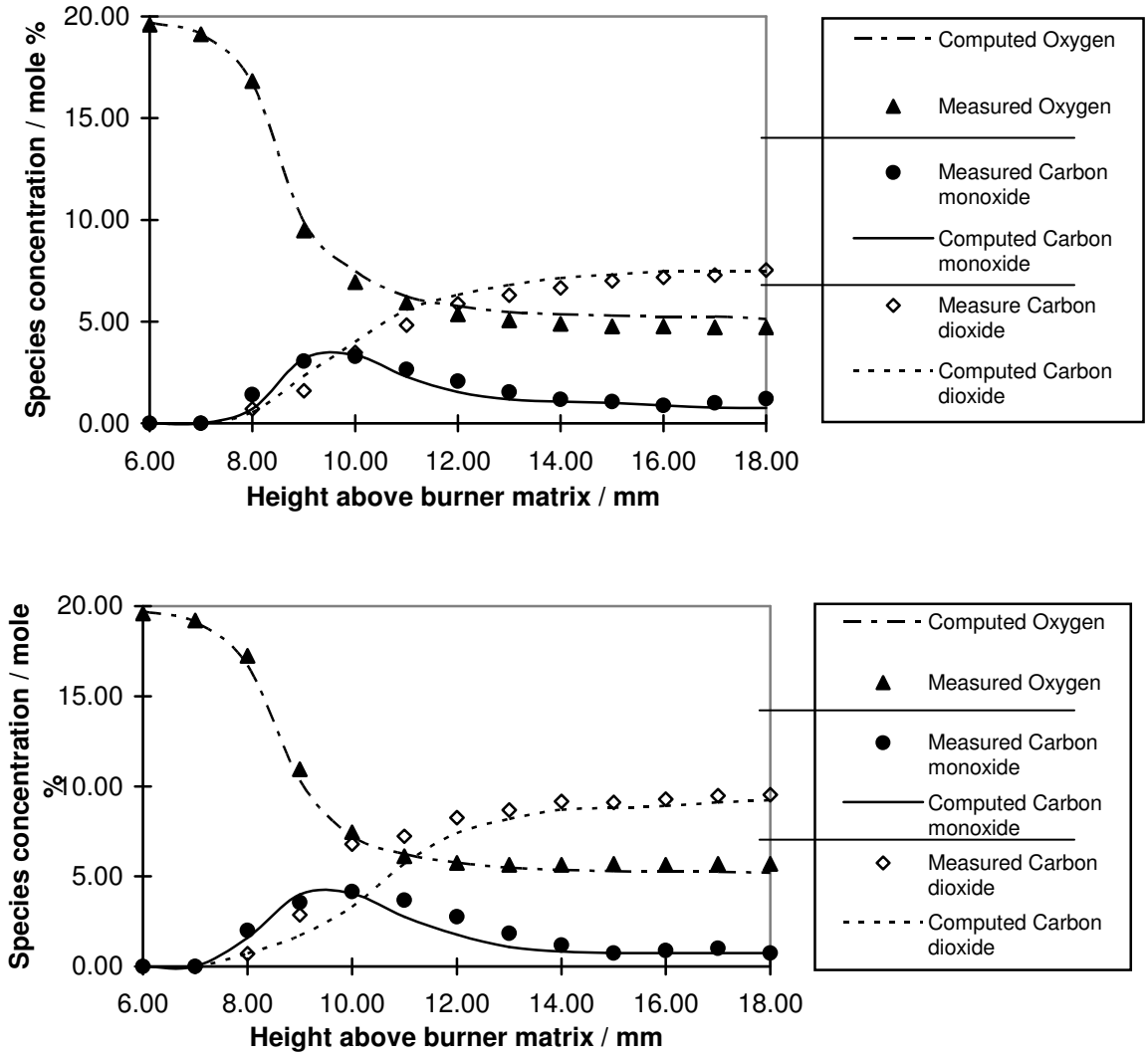

Fig 3 Measured and computed O_2, CO, CO_2 for a methane-air flame equivalence ratio, ϕ =0.7 at 0.160 atm. Seeded with graphite at a concentration, Fc of 9.80×10^{-3} and 2.60×10^{-2}

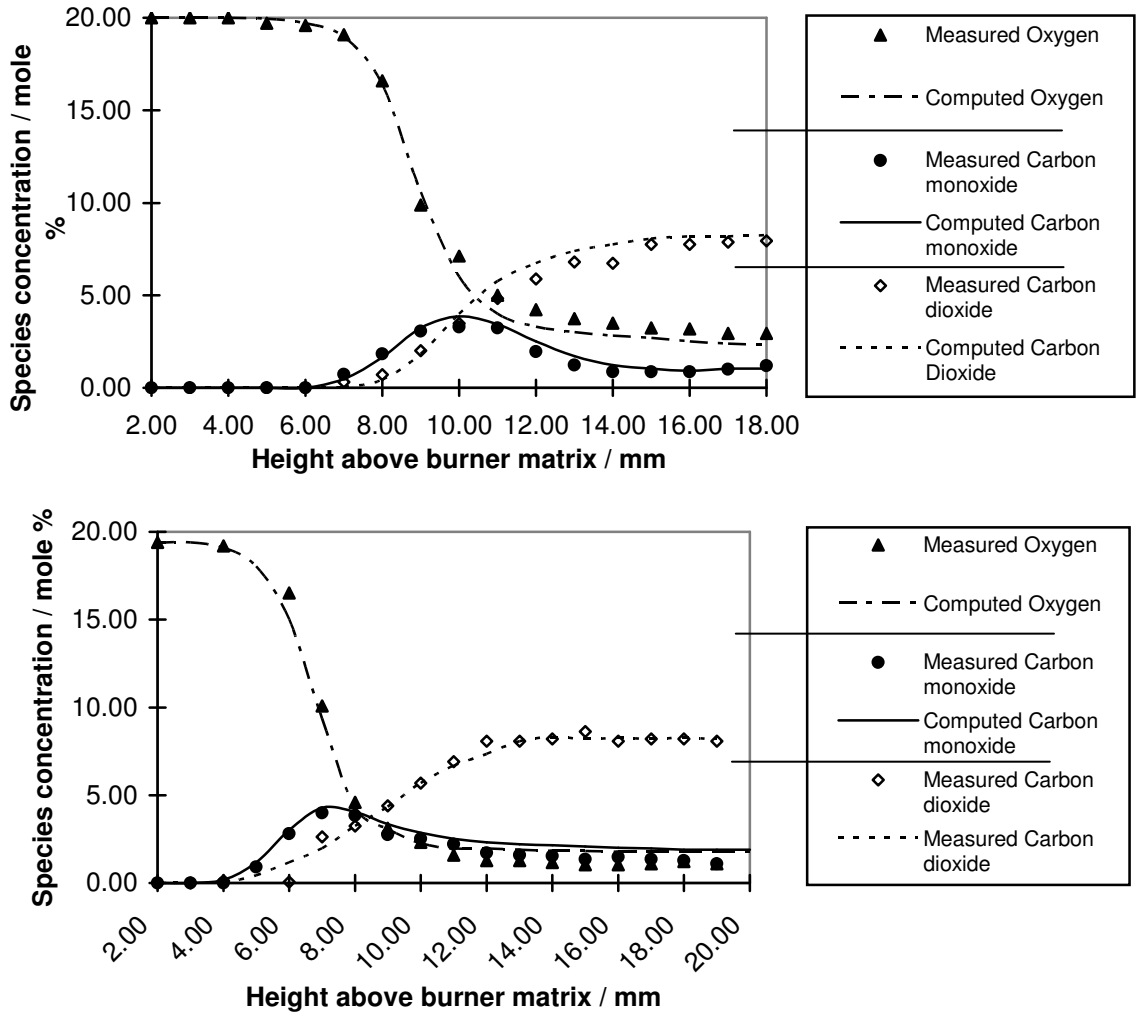

Fig 4 Measured and computed O_2, CO, CO_2 for a methane-air flame equivalence ratio,ϕ=0.7 at 0.160 atm. Seeded with graphite at a concentration, Fc of $3.92x10^{-2}$

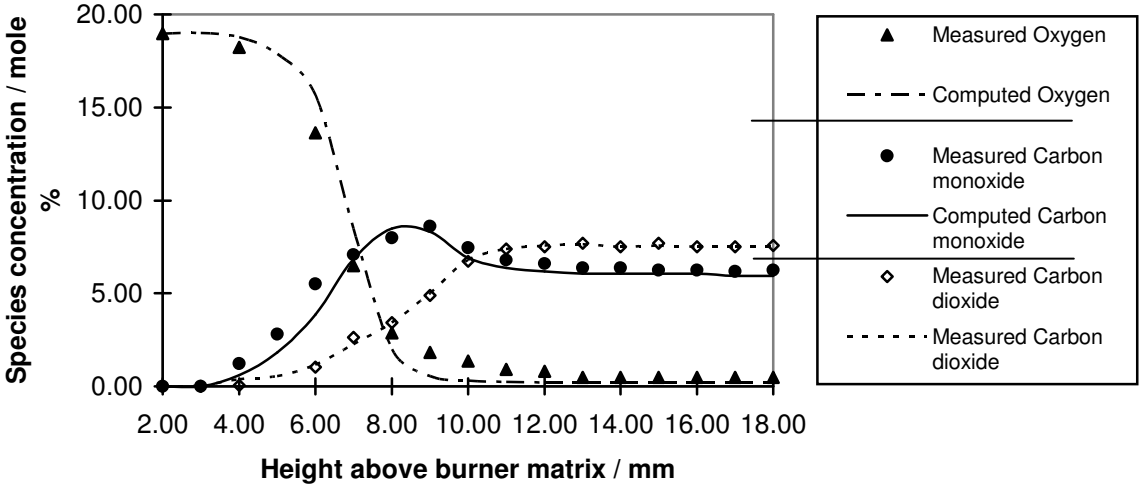

Fig 5(a) Measured and computed O_2, CO, CO_2 for a methane-air flame equivalence ratio, ϕ=1.2 at 0.160 atm. Seeded with graphite at a concentration, Fc of $1.60x10^{-2}$

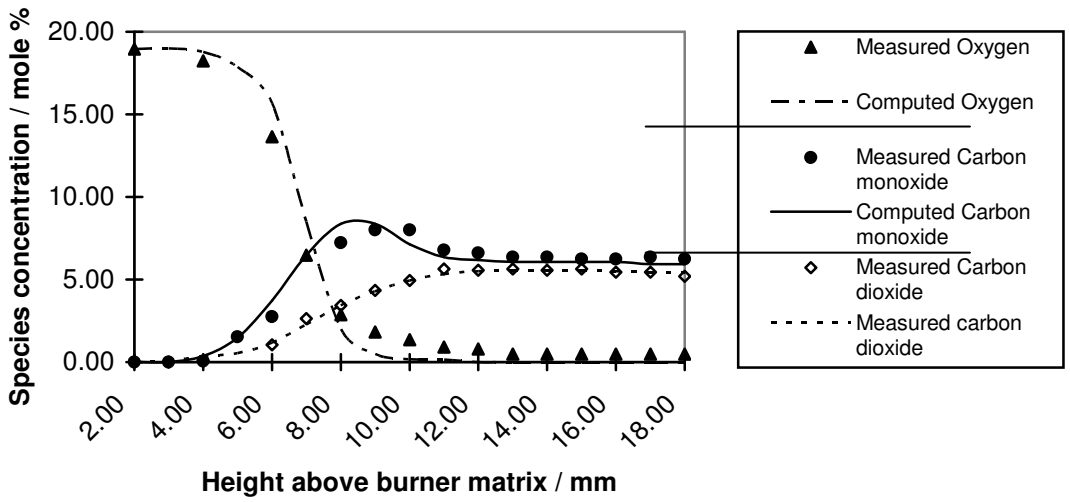

Fig. 5(b) Measured and computed O_2, CO, CO_2 or a methane-air flame equivalence ratio, ϕ =1.2 at 0.160 atm. Seeded with graphite at a concentration, Fc of 4.35×10^{-2}

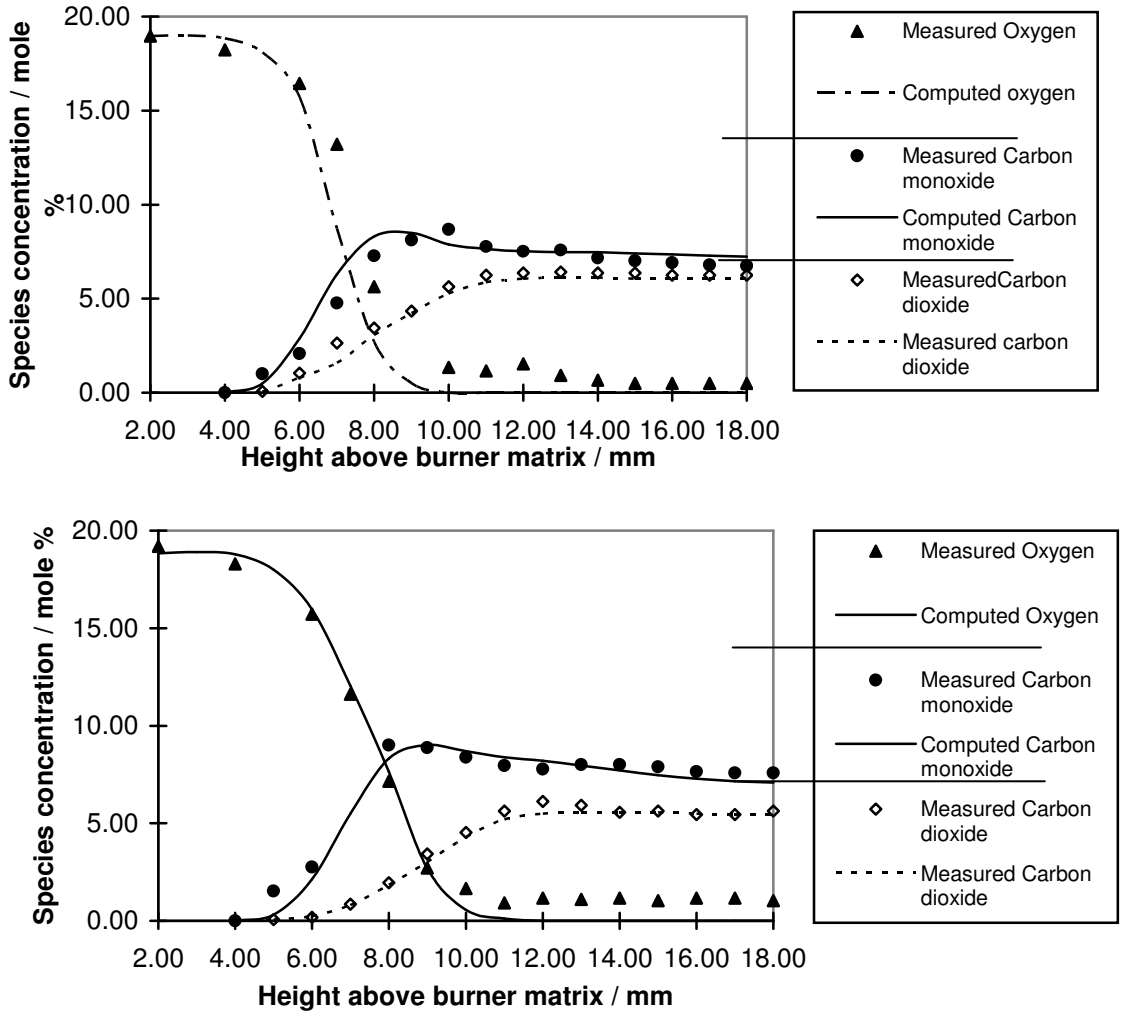

Fig 6 Measured and computed O_2, CO, CO_2 for a methane-air flame equivalence ratio, ϕ=1.2 at 0.160 atm. Seeded with graphite at a concentration, Fc of 6.54×10^{-2} and 9.79×10^{-2}

Figures 7 and 8 summarise the effects of graphite addition on the maximum concentrations of the radical species OH, O and H and on the maximum CO concentration, together with burning velocity for CH_4 – air flames with ϕ = 0.7 and 1.2. The situation for ϕ = 0.7 is that there is an initial increase in the maximum OH concentration with graphite concentration and this peaks when F_c = 0.013. Thereafter, there is a slight fall in the concentration with increase in F_c. The maximum concentrations of H and O soon fall with increase in F_c. These trends are more marked for ϕ = 1.2, as shown in Fig. 8 where all maximum concentrations fall with any addition of graphite.

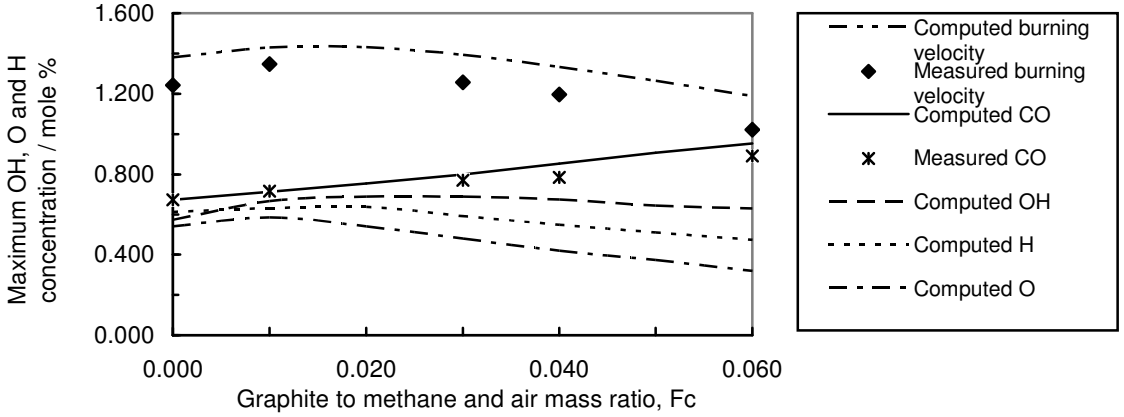

Fig 7 Effect of graphite loading on burning velocity, and computed maximum concentrations of OH, O, H, CO in dry molar percentage for a methane-air flame equivalence ratio, ϕ = 0.70 at 0.160 atm

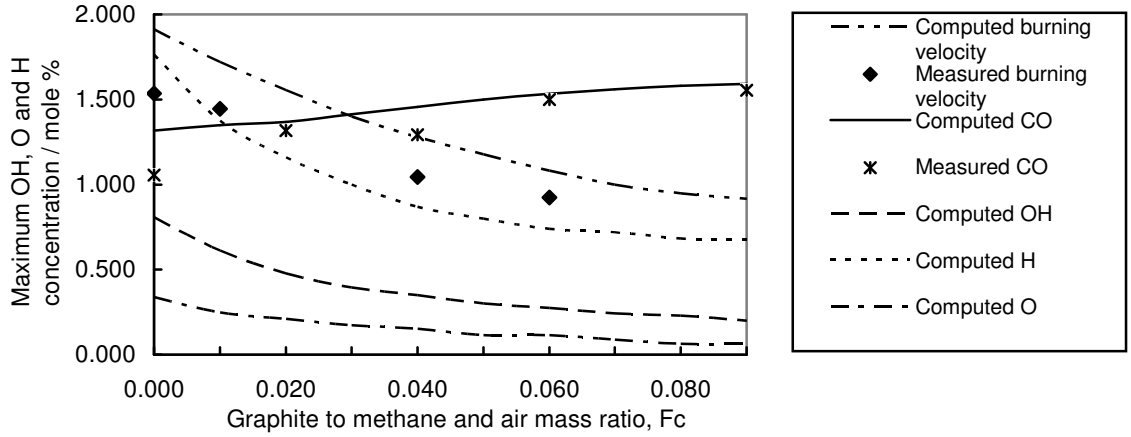

Fig 8 Effect of graphite loading on burning velocity, and computed maximum concentrations of OH, O, H, CO in dry molar percentage for a methane-air flame equivalence ratio, ϕ = 1.2 at 0.160 atm

The initially observed increases in the maximum concentration of H, OH and O in the lean flame are attributed to the production of these via reactions (28) – (31) and (35) – (36) in Table 2. For ϕ = 0.7 the excess O_2 enhances reaction (28) that leads to both increased OH and O concentrations. Reactions (35) and (36) explain the marked increase in CO concentration with F_c and the increase in H concentration, to which reaction (31) also contributes. For the rich flames, because of the limited amount of O_2, these reactions are limited and the relative increase in CO concentration is relatively less, although the maximum concentration of CO increase with F_c for both lean and rich flames. It is of particular interest to note how the changes in burning velocity follow those in maximum OH

concentration. Only with the lean mixtures is there an initial increase in burning velocity with F_c.

5. CONCLUSIONS

The combustion of pulverised coal is exceedingly complex with a vast number of variables; this study has attempted to control the velocity by decoupling some of the variables by undertaking the oxidation of fine graphite in laminar methane-air burning in one dimensional methane-air flame. This is viewed as a contribution to the understanding of the more complex practical phenomena. The burning of the graphite is equivalent to the burning char which is one of the important rate processes in pulverised coal combustion. Aspects of this process have been simulated in experimental and computational studies of graphite oxidation in methane – air flames. The catalytic oxidation mechanism for the reaction of carbon has been coupled with the gas phase kinetic scheme.

The small size of graphite particles and the low pressure used in the studies ensured that the graphite reactions were chemically, and not diffusion, controlled. The chemical kinetics of graphite oxidation are coupled with methane oxidation kinetics in a mathematical model of the ultra – fine graphite – methane – air flame. The application of the same is reported in other work (John, 2005)

Validation of this model was through measurements of burning velocity, gas velocity, gas temperature, and concentrations of CO, CO_2, and O_2 at low pressure. The low pressure was of the great advantage of extending the reaction zone since the reaction zone thickness is inversely proportional to pressure (Hirschfeder et al, 1985) and thus facilitated sampling through the flame and, hence, kinetic studies. In general, there was good agreement between the measured and computed results. The imposed one dimensionality of the model might explain some discrepancies, particularly with regard to the over – prediction of gas velocities. For heavily seeded flame there is also the possibility of some heat loss to the burner matrix. There are some chemical kinetic uncertainties for rich flames. These appear to be somewhat aggravated by the addition of seed.

6. REFERENCES

Barratt, D.J. and Roberts, P.T., 1989
The suitability of ultrafine coal as an industrial boiler fuel, Combust Flame, vol. 77 pp. 51 – 68

Backreedy, R.I, Jones J.M., Pourkashanian and Williams A., 2002
Modelling the Reaction of Oxygen with Coal and Biomass Chars, Twenty Ninth Symposium (International) on Combustion, The Combustion Institute, Pittsburgh, pp 694-703

Bradley, D., Z. Chen, Sherif S.E., Habik, S.E. and John G.R., 1994
Structure of Laminar Premixed Carbon Methane-Air Flame, Combust Flame, Volume 96, Number 1 and 2, pp 80-96

Bradley, D., and Lee, J.H.S., 1984
The mechanisms of propagation of dust flames *First International Colloquium on Explosibility of Industrial Dusts, Baranow, Polish Academy of Sciences, part 2, pp. 220-224.*

Bradley, D., Dixon – Lewis, G. and Habik, S. El – Din, and Mushi, E.M.J., 1985
The oxidation of graphite powder in flame reaction zones

Twentieth Symposium (International) on Combustion, The Combustion Institute, Pittsburgh, pp. 931-940.

Bradley, D., Habik, S. and Swithenbank, J.R., 1986
Laminar burning velocities of Methane – air – graphite mixtures and coal dusts, Twenty – first symposium (International) on Combustion, pp. 249 – 256, Combustion Institute.

Bradley, D., Dixon – Lewis, G. and Habik, S. El – Din, 1989
Lean flammability limits and laminar burning velocities of CH4 – air – graphite mixtures and fine coal dusts, Combust Flame, vol 77, pp 41 – 50

Bradley, D., Dixon – Lewis, G. and Habik, S. Kwa, L.K. and El – Sherrif, S., 1991
Laminar Flame Structure and Burning Velocities of Premixed Methanol – Air Combustion and Flame, Vol. 85, pp. 105 – 120

Chen, Z.M., 1990
Turbulent dust explosions, Ph.D Thesis, Department of mechanical Engineering, The University of Leeds

Dixon-Lewis, G., 1984
Computer modeling of combustion reactions in flowing systems with transport In Combustion Chemistry, (W.C. Gardiner Jr. Ed), Springer-Verlag, New York, Chapter 2

Dixon – Lewis G., Bradley, D. and Habik S., 1987
Burning of coal and organic dusts in Air, Archivum combustionis, vol. 7, pp. 85 – 98

Dixon – Lewis, G. Bradley, D. and Habik, S. El – Din, 1991
Oxidation rates of Carbon Particles in methane –Air Flames. Combust Flame; 86, 12 - 20.

Hirschfelder J.O, Curtis, C.F and Bird R.B., 1985
Molecular Theory of Gases and Liquids, John Wiley & Sons, Inc. Library of Congress Catalog Card Number; 54-7621

JANAF, 1977
Thermochemical Tables, NS RDS – NBS 37 National Bureau of Standards, Washington

John G.R., 1991
Fundamentals of Pulverized Coal Combustion, PhD. Thesis, Department of Mechanical Engineering, University of Leeds, U.K

John G.R., 1995
Prediction of Coal Particles Temperature Under a Variety of Combustion Conditions, 3rd Asia-Pacific International Symposium on Combustion and Energy Utilization, Hong Kong, Pg 691-696

John G.R., 2005
The Role of Gas Phase Linetics in the Heat Release Rate of Utrafine Char Oxidation, East Africa Journal of Engineering, Vol 8, No 1, pp 15-27

Mulcahy, M.F.R. and Smith, I.W., 1969
Kinetics of Combustion of Pulverised Fuel, a review of Theory and Experiment Reviews of Pure and Applied Chemistry, Vol. 19, pp. 81-107

NASA, 1984
Tables of coefficient for NASA polynomials, Appendix C in Combustion Chemistry, W.C. Gardiner Jr. Ed, Springer-Verlag, New-York, Report 1300, pp 257

Ruksana Moreea-Taha, 2000
Modelling and Simulation for Coal Gasification, IEA Coal Research, ccc/42 ISBN 92-9029-354-3

Smoot, L.D and Smith, P.J., 1990
Coal Combustion and Gasification, The Plenum Chemical Engineering Series

Williams A., Pourkashanian, M., and Jones, J.M., 2001
Combustion of Pulvirised Coal and Biomass Progress in Energy and Combustion Science, Vol. 27, pp 587-610